Monsoon Flood Boundary Delineation and Damage Assessment Using Space Borne Imaging Radar and Landsat Data

Marc L. Imhoff and *C. Vermillion*
NASA/Goddard Space Flight Center, Greenbelt, MD 20771

M. H. Story
Science Applications Research Corporation, Lanham, MD 20706

A. M. Choudhury and *A. Gafoor*
Space Research and Remote Sensing Organization, of Bangladesh, Dhaka, Bangladesh

F. Polcyn
Environmental Research Institute of Michigan, Ann Arbor, MI 48107

ABSTRACT: Space-borne synthetic aperture radar (SAR) data acquired by the Shuttle Imaging Radar-B (SIR-B) Program and Landsat Multispectral Scanner Subsystem (MSS) Data from Landsat 4 were used to map flood boundaries for the assessment of flood damage in the Peoples Republic of Bangladesh. The cloud penetrating capabilities of the L-band radar provided a clear picture of the hydrologic conditions of the surface during a period of inclement weather at the end of the wet phase of the 1984 monsoon. The radar image data were digitally processed to geometrically rectify the pixel geometry and were filtered to subdue radar image speckle effects. Contrast enhancement techniques and density slicing were used to create discrete land-cover categories corresponding to surface conditions present at the time of the shuttle overflight. The radar image classification map was digitally registered to a spectral signature classification map of the area derived from Landsat MSS data collected two weeks prior to the SIR-B Mission. Classification accuracy comparisons were made between the radar and MSS classification maps, and flood boundary and flood damage assessment measurements were made with the merged data by adding the classifications and inventorying the land-cover classes inundated at the time of flooding.

INTRODUCTION

SINCE THE LAUNCH of the first Earth Resources Technology Satellite, later renamed Landsat, synoptic views of the Earth's surface from space have been tremendously useful tools in the discovery, survey, and management of the Earth's resources and environment. The developing countries of the world have found this data source extremely helpful in development planning, especially in the absence of photographic aerial survey coverage. For many of the developing nations in the world, however, a severe seasonal hiatus has existed in the acquisition of both aircraft and satellite acquired image data. The thick and widespread cloud cover that accompanies the wet phase of the monsoon cycle has historically prevented the acquisition of synoptic survey data for many regions of the globe during one of the most physically and environmentally stressful periods of the year.

It is during the wet phase of the monsoon that planners and agriculturists must see how their various projects are interacting with the landscape and the weather. It is during the heavy rains that mistakes or oversites in infrastructural planning will manifest themselves, flood damage will be evident, and important information about crops must be collected for making yield estimates. The advent of synthetic aperture radar imaging systems has presented a unique opportunity for monsoon countries to synoptically observe their environment during this important season.

The project described here was a first attempt at utilizing SAR image data for making a survey of flood boundaries in a developing country which has a monsoon climate. The project was carried out in the Peoples Republic of Bangladesh as part of a cooperative program between the National Aeronautics and Space Administration (NASA) and the Bangladesh Space Research and Remote Sensing Organization using SAR data collected by the Space Shuttle Challenger as part of NASA's Shuttle Imaging Radar-B (SIR-B) program.

BACKGROUND

Attempts at making flood boundary and flood damage surveys using Landsat have been made with varying success. Thomson and Prevost (1983) used Landsat and other satellite data in West Africa as input to agrometeorological models and Berg and Gregiore (1983) used Landsat data in West Africa to map the areal extent of post monsoon flooding. In each case mapping of flood boundaries was reported limited by spectral confusion between the water and burned land and obscuring vegetative cover, respectively. Bhavsar (1984) reports the advantageous use of Landsat data for mapping surface water and flood plains in India and Raungsiri *et al.* (1984) used Landsat to map floods in the Mun-Chi river basin area in Thailand.

In all of the above mentioned instances, because of the sensors used, the success of the surveys was contingent on the absence of cloud cover. In most cases the timely acquisition of flood data is prevented by obscuring cloud cover. This is an especially severe limitation in monsoon countries where flooding results from widespread precipitation over relatively long periods of time.

The use of SAR systems as a solution to the cloud cover problem has shown great promise. With the advent of Seasat, imagery from its L-band synthetic aperture radar was explored for its potential in flood mapping and water resources evaluation. Aircraft systems have also been examined for mapping floods and lowland vegetation. Lowry *et al.* (1979) had some success in using aircraft mounted X- and L-band SAR systems to map flood boundaries in Manitoba, Canada.

Radar imaging systems also showed that they were capable of allowing delineation of flood boundaries beneath vegetation canopies, having been verified in diverse situations. Waite and MacDonald (1971) first noted the "penetration" phenomenon in "leaf off" conditions in Arkansas using Ka-band radars. MacDonald *et al.* (1980) and Waite *et al.* (1981) later noted it in similar circumstances from Seasat. This phenomenon was also

PHOTOGRAMMETRIC ENGINEERING AND REMOTE SENSING,
Vol. 53, No. 4, April 1987, pp. 405–413.

0099-1112/87/5304–405$02.25/0

noted by Krohn *et al.* (1983), Ormsby *et al.* (1985), and Imhoff and Story (1986) at a variety of incidence angles in fully leafed forest conditions in eastern Maryland, Virginia, and the Peoples Republic of Bangladesh, respectively.

The actual application of SAR for flood mapping, however, has been frustrated due to a lack of regularly available data such as might be achieved using space borne SAR platforms. Aerial acquisition of radar data has been used in many tropical areas for a variety of applications, but the perturbations of bad flying weather and the limited areal extent achievable by aircraft acquisition has prevented this option from being implemented as a reliable source of surface data during the monsoon.

In October 1984 digital radar image data were collected over the Gangetic Plain in the Peoples Republic of Bangladesh. The data were used for delineating flood boundaries, mapping land use, and determining flood damage. The experiment was designed to demonstrate the rapid assessment survey potential of spaceborne SAR by providing an immediate source of flood and flood-damage survey data. The conventional method of compiling this sort of information for many developing countries consists of a very time consuming process of collection and collation of point data usually retrieved through the postal system. While this methodology provides accurate data, it is quite slow in its application (output of reports often take two to three years from time of collection) and, as point data, it is limited in its areal extendability. The classifications rendered from the satellite data in this study, therefore, were designed to be relatively simple or broad in definition to serve as a rapid assessment of flood inundation areas for the development of damage assessments.

GEOGRAPHY AND DATA

The flood prone nature of its geomorphology and the size of its population make Bangladesh one of the most difficult ecosystems in the world to manage. Located between 21° 45′ and 26° 40′ north latitude and 88° and 92° 30′ east longitude, Bangladesh lies on the Tropic of Cancer between India and Burma (Figure 1). Most of the country consists of the flood plains of the Ganges, Brahmaputra, and Meghna river systems. With a total area of 144,000 square kilometres and a population in excess of 97 million, Bangladesh is one of the most densely populated nations in the world (Rashid, 1981). Every year this region experiences an extreme cycle of dehydration and flooding. During the winter precipitation is limited by the Siberian high pressure system and during the summer months flooding occurs as the major river systems, swollen with the Himalayan snowmelt, are further fed by heavy monsoon precipitation.

The Space Shuttle Challenger collected digital SAR data over Bangladesh in a northeast by southwest swath approximately 50-km wide extending from the Bay of Bengal in the south to the Jillong Plateau of northeastern India in the north on 11, 12, and 13 October 1984. The SAR data used in this analysis was acquired on 12 October through heavy cloud cover using an incidence angle of 46 degrees with a spatial resolution of 33.8 m in azimuth and 19.8 m in range.

Landsat MSS data were acquired bout 15 days prior to the SIR-B overflight via the Landsat receiving and processing facility in Thailand. Aerial photo coverage was acquired two years earlier (see Table 1).

The area selected for analysis is located on the Ganges River centered on the town of Chandpur in the Comilla District of Bangladesh and includes the eastern part of the Barisal District at the confluence of the Meghna and Padma rivers (Padma is the Bengladeshi name for the Ganges south of the Ganges-Brahamputra convergence) (Plate 1). The area consists entirely of river and densly populated river flood plain under heavy rice cultivation.

The radar and Landsat data sets were digitally processed using the VAX based Land Analysis System (LAS) located at Goddard Space Flight Center in Greenbelt, Maryland.

TABLE 1. DATA SETS.

SIR-B Data					
Data Take # DT	Date Acquired	Incidence Angle	Bit/Sample	Resolution (m) Range	Azimuth
104 (GMT)	Oct. 11, 1984 20:48:21.5	46°	5	19.8	33.7

MSS Data			
Scene #	Path, Row	Date	Receiving Facility
4080403494	137, 44	27 Sep. 1984	Thailand

Aerial Photography		
Type	Scale/Resolution	Date of Completion
Color IR	1:30,000	March 1983

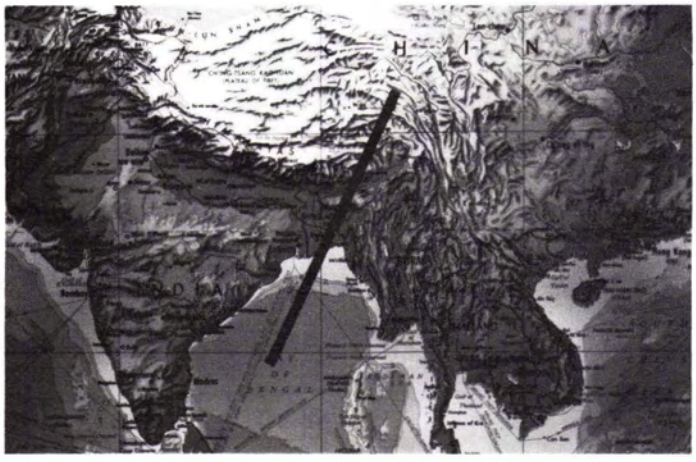

FIG. 1. Geographic location of the Peoples Republic of Bangladesh with location of SIR-B image track.

PLATE 1. Location of Chandpur study area shown on a dry season Landsat MSS false color composite mosaic (courtesy of the World Bank). The Sundarbans mangrove forests can be seen at the lower left part of the mosaic and the forested Chittagong Hill Tracts can be seen at the right side of the mosaic. Most of Bangladesh is under intense cultivation, as can be seen in the center part of the mosaic.

OBJECTIVES AND APPROACH

The basic objective of this study was to demonstrate the potential of radar imaging systems for flood boundary delineation and to analyze their ability for making rapid broad definition land-use classifications for future use in aiding infrastructural and agricultural planning and flood damage survey programs in monsoon countries.

The approach used was one of simple temporal comparison. Land-cover classification maps derived from Landsat and SIR-B data acquired at different times were compared to derive flood water inundation measurements. In this rare instance, a Landsat MSS scene was acquired on 27 September 1984, and showed considerable flooding still in effect as a result of monsoon and storm activity. The Landsat data, therefore, were used to define land-cover classes present during a flooded condition. The SIR-B data were acquired some 5 days after the Landsat acquisition when most of flood waters had receeded. As a result, it was used to define the natural boundary of the water-dry land interface in a non-flooded condition. Subsequently, a comparison between the two data sets could yield areal measures of land-cover classes that were subjected to flooding.

The Landsat MSS data were classified using an unsupervised Euclidean distance classification algorithm, and class assignments were made through comparison to ground truth. Land-cover classification on the SIR-B radar image was achieved using spatial smoothing filters, contrast enhancement, and density slicing techniques. Once the land-cover classifications were derived, the data were geometrically rectified and merged for information content comparison and temporal change detection analysis.

The classifications derived for both the Landsat and SAR data were assessed for accuracy through comparison to 1:24,000-scale color IR aerial photographs. The accuracy assessment was based on a selection of sample points on the classified images using a systematic dot grid. The sample point locations were then defined on coregistered aerial photogrpahs using the LAS image display, and the agreement between the categories shown on the classification maps and the actual target feature shown by the photography was recorded in a contingency table. Two accuracy values were computed from the contingency tables. The percent correct value was computed by summing the diagonal of the matrix and dividing the value by the number of samples.

The other measure of accuracy used was the KAPPA statistic. The KAPPA statistic is a nonparametric measure of the difference between the actual agreement of the classification and the agreement achieved by chance (Congalton *et al.*, 1983). The KAPPA statistic was computed by

$$\text{KAPPA} = \frac{N\sum_{i=1}^{r} \chi_{ii} - \sum_{i=1}^{r} \chi_{it}\,\chi_{ti}}{N^2 - \sum_{i=1}^{r} \chi_{it}\,\chi_{ti}}$$

where

N = number of samples,
χ_{ii} = diagonal elements,
χ_{it} = row total, and
χ_{ti} = column total.

The classified images were then compared by using a Z statistic to determine if they were significantly different. The Z statistic is computed by

$$Z \text{ statistic} \sim \frac{\hat{K}_1 - \hat{K}_2}{\sqrt{\hat{\sigma}_1^2 + \hat{\sigma}_2^2}}$$

where $\hat{\sigma}$ is the variance of KAPPA calculated at the 95 percent confidence level.

If the value of the Z statistic is greater than 1.96, it was held that there was a significant difference between the classifications compared at the 95 percent confidence level.

In order to make areal inundation projections as a function of measured river level, the final classifications showing flooded and non-flooded land categories were compared to data obtained from an operating river guage for this area showing river level in centimetres at a point in the Ganges River just outside the town of Chandpur. Readings for this station were taken at the times of the Landsat and SIR-B overflights.

RESULTS AND DISCUSSION

At the time of the Landsat acquisition monsoon and storm induced flooding was still in effect in the Chandpur study area (Plate 2) and the northern parts of Bangladesh (Plate 3). The Landsat acquisition was quite fortunate due to the high cloud cover usually present during this period. At the time of SIR-B data acquisition, most of the flood waters in the Chandpur area had receeded completely. In the northern areas, however, the presence of large amounts of surface water could still be noted.

Landsat Classification and Analysis

A combined supervised and unsupervised Euclidean distance classifier was used to derive the land-cover classification for the Landsat image. Not surprisingly, the land-cover categories extracted from the MSS data were relatively simple or broad in definition due to its limited spectral and spatial resolution (Plate 4a). With respect to target land-cover features, the MSS data proved to be somewhat inadequate for defining important land-cover categories in this type of terrain with its typical patterns of land use. Even with the broad categories used here, the classification accuracies computed for each individual land-cover category were not exceptionally high, and the overall classification accuracy achieved using the Landsat MSS fell short of 80 percent (Table 2).

The MSS data were useful for visually identifying flooded areas but, when used for digital classification, several shortcomings were noted.

A primary problem occurred as an apparent inability to spectrally separate the village class from the agricultural surfaces. From a disaster management point of view, this limitation was considered important as it hindered the determination of separate estimates of infrastructural versus agricultural flood damage. The reason for the confusion, however, is readily apparent. Many of the dwellings in this part of Bangladesh, as in many other nations living primarily on rice agriculture, are distributed throughout the agricultural fields as extensions of a raised dike system which serves to separate the various irrigated fields and provides a sort of transportation conduit to the various households, villages, and commercial centers. Many of these households are also distributed as single points or clusters in the larger fields and are not necessarily connected to the diking system. While these dikes and households represent a considerable area when added together (approximately 10 percent of total agricultural area in this region as estimated by areal count from radar data), their natural spatial geometry and distribution make them hard to distinguish at coarser resolutions. A sensor spatial resolution of at least 30 metres or so would be required to distinguish them as the dikes are narrow (less than 30 m in most cases) and many of the separate households or

TABLE 2. CLASSIFICATION ACCURACY ASSESSMENT FOR LANDSAT MSS DATA.

Landsat MSS	Agriculture/ Village	Flooded Land	Water	% Accurate
Agriculture/Village	54	3	16	73.97
Flooded Land	19	83	26	64.84
Water (non-flood)	0	0	79	100.00
			Overall accuracy	77.14

Total Samples = 280
Diagonal Total = 216
Kappa Statistic = 0.5811

clusters are small (between 5 and 30 m). Because most of the larger components of the diking system and villages are covered in shade and fruit trees and vegetable crops, and the dwellings are made of thatch, feature separation relying on spectral separability between these areas and the agricultural fields was also diminished. As a result, it became impractical to derive signature statistics capable of separating all but the largest villages from the rice and jute fields using the MSS data, and subsequently the two features were combined to form the category Village/Agriculture.

The spatial resolution limitations in the MSS also caused errors in classification near the boundary areas where agricultural fields were immediately adjacent to flooded areas, rivers, and ponds. As a result, classification accuracies even for a combined Village/Agricultural category using the MSS data fell short of 74 percent.

With regard to the delineation of flooded zones, the spatial limitations of the MSS were further exacerbated by some spectral similarities between these areas and the heavily turbid river areas, turbid water in flood irrigated agricultural fields, and the nonvegetated soil surfaces of the village and dike areas. In each of these cases the presence of large quantities of similar or identical clay and silt material made these features more difficult to separate, thus driving the accuracy of the classification for Flooded Land down to about 64 percent. The overall accuracy for the Landsat data classification was 77 percent and the KAPPA statistic calculated for the Landsat land-cover classification was 0.5811.

Although these accuracies may be considered low for many applications, they can be a revelation in the absence of better data. For many monsoon countries, little or no high resolution synoptic data exists during the monsoon, and even with the advent of Landsat TM and the French SPOT data, cloud free acquisitions during the wet phase of the monsoon are rare. This was also the case in this study. No data other than the MSS data used here existed for this area during the time interval of interest, and the accuracies of classifications derived by the extension of low density ground acquired point data would almost certainly be less than those achieved using the Landsat MSS data.

Radar Data Analysis

Analysis of the radar data for the Chandpur area took place in three stages. The first stage consisted of converting the slant range 4 look imagery to ground range and resampling to create square display pixels. The second stage consisted of passing a 3- by 3-pixel median filter over the data to smooth out some of the remaining image speckle, and the third stage consisted of contrast enhancement and supervised density slicing to create the broad category land-cover classification.

The radar derived landcover classification accuracies were better than those achieved by means of the MSS data (Table 3, Plate 4). The smaller spatial resolution of the radar and the physics behind its functioning allowed for good definition of land-cover classes useful for flood boundary and damage assessment.

The diking system and the villages and household clusters prevalent in the area were well defined on the imagery and were, in most cases, clearly separable from the agricultural surfaces. This useful phenomenon can be primarily attributed to a corner reflector effect resulting from the close proximity of specular surfaces (non-turbulent water in the rice fields) and raised surfaces (the dikes and dwellings). Radar energy arriving near the edges of the irrigated or flooded fields reflects off the water away from the radar antenna only to strike the raised earthworks which reflects the energy to the radar (Figure 2). The water filled fields, therefore, appear specular or as dark areas on the image and the raised dikes and villages appear as bright areas. The net effect is one of enhancement where the dike works around the rice fields and the households are clearly delineated. Similarly, abrupt changes in topography (>23 cm in height with steep slopes of 45 degrees and up) caused by river meander scars and terracing, etc., were also quite visible. This latter effect was found useful for the mapping of flood plain levels.

TABLE 3. CLASSIFICATION ACCURACY ASSESSMENT FOR SIR-B RADAR DATA.

SIR-B Radar	Reference Aerial Photography				
	Village	Agriculture	Water	Scrub Vegetation	Percent Accurate
Village	63	13	0	0	82.89
Agriculture	12	67	6	0	78.82
Water	0	0	70	12	85.36
River Vegetation	0	0	0	42	100.00
				Overall Accuracy	84.91%

Number of samples = 285
Diagonal Total = 242
Kappa Statistic = 0.7947

The classification accuracy for the class representing village and dike areas was around 83 percent. The real accuracy for this category is probably even better, but the temporal difference between the aerial photography and the SIR-B overflight caused errors to be registered where newly erected dikes and household structures were delineated on the radar but were still in agricultural use during the time that the aerial photography was taken two years earlier.

The turbidity of the water has no direct effect on radar backscatter, so the delineation of flooded versus ponded or flood-irrigated areas using silt content was not possible using the radar data. Some confusion was also apparent between flood irrigated agricultural crops and water. This occurred wherever there was inadequate crop growth above the water line to create enough backscatter to offset the specular response characteristics of open water, or where land areas present during the time of the aerial photography had eroded away by the time of the SIR-B overflight. Despite these errors, the classification accuracy for the radar derived class representing Water was 85 percent.

Because there was little or no significant flooding in effect at the time of the radar acquisition, the radar derived class boundaries for water became the means by which to separate flood versus nonflood water features on the MSS.

The classification of agricultural areas using the L-band radar also suffered some limitations. A few of the areas classified as Agricultural Land on the radar were determined to be Village on the photography. The two most likely causes for this confusion are (1) mature jute or rice crops may have created strong backscatter responses similar to those created by small earth works and/or (2) some of the smaller households or earthworks that were oriented in a direction parallel to the range of the radar had reduced backscattering cross-sections and appeared at an intensity on the image similar to those of crop areas. In either case accurate mapping of agricultural crops was limited using the radar data, although the classification accuracy achieved for defining crop areas was 78 percent. Scrub areas near the river banks were classified at 100 percent accuracy. This was primarily due to the fact that these areas were seen by the radar as flooded "forests" and had characteristically very bright returns.

Another source of potential confusion in the classification of the radar data for land-cover was the problem of turbulent water. Wind induced wave fronts on the river, flooded zones, or in the deeper flood irrigated fields may become large enough to induce slight increases in the backscatter response for these areas, making them appear similar to crop areas. Fortunately, the winds were calm during the time of SIR-B data acquisition used in this analysis, but the effect was noted on a SIR-B image of the same area taken one day later during a storm (Plate 2c.).

Even with all the sources of confusion mentioned above, the classification accuracies for the radar derived land-cover classes were acceptable. The overall accuracy of the SIR-B radar classification was about 85 percent as compared to the overall accuracy of 77 percent achieved using the Landsat MSS.

The KAPPA statistic calculated for the SIR-B derived land-cover classification was 0.7947. When the KAPPA statistics for the two

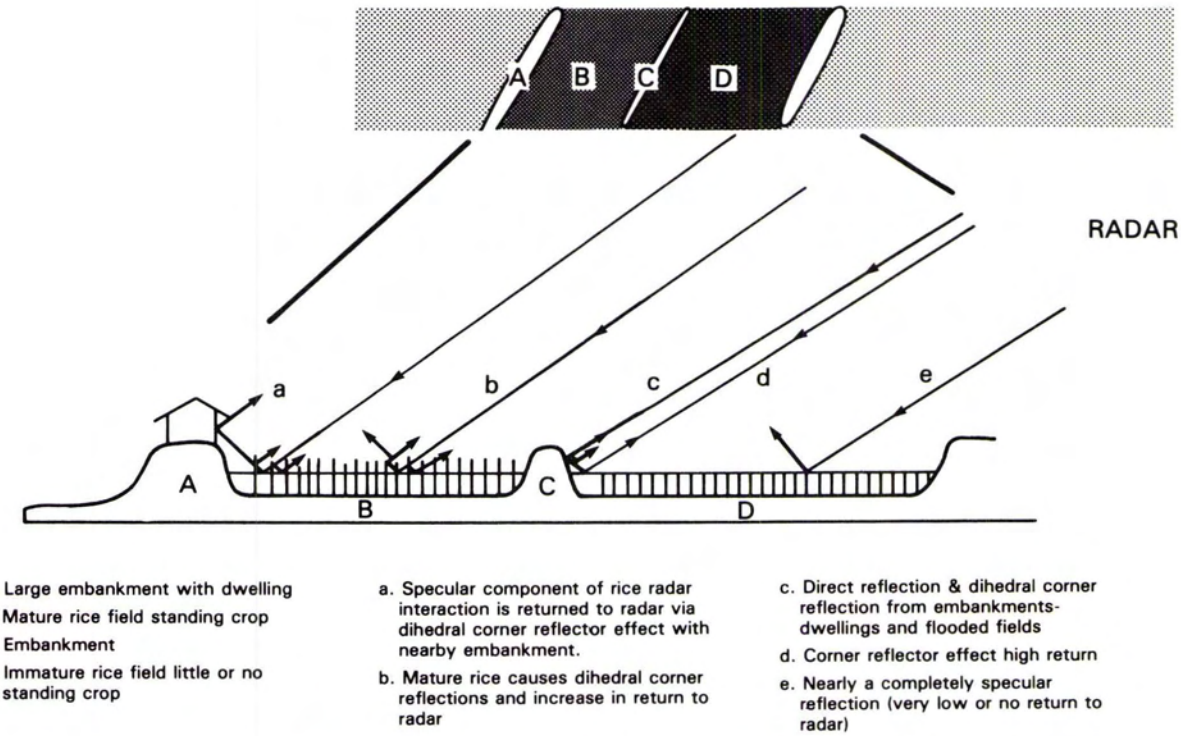

FIG. 2. Radar reflectance characteristics of rice agriculture — village areas.

TABLE 4. FLOOD AREA INUNDATION SUMMARY (HECTARES).

SIR-B (Oct. 12, 1984)	Landsat MSS (27 Sep. 1984) Water (non-turbid)	Flood Water (very turbid)	Agriculture/ Village
Water (non-flood)	42,062	6,098	7550
Agriculture	*25,483	*33,069	75,624
Village	* 520	* 1,948	11,439
Scrub Vegetation	* 381	* 1,638	494

Total area 206,306

*The sum of these components were used to estimate number of hectares of land flooded by river overflow on 27 Sep. 1984.

A total of 63,039 hectares in the survey area (206,306 ha. total) were considered flooded on 27 September 1984. Of that, approximately 58,552 hectares were estimated to be agricultural land, 2468 hectares were homesteads or other infrastructure, and 2019 hectares were scrub lands at the river margins.

classifications were input to the Z test, the resulting Z statistic computed as 4.5937, indicating that there was a statistically significant difference between the classification accuracies at the 95 percent level of confidence.

RADAR-LANDSAT DATA MERGER ANALYSIS

In order to make estimates of land-cover types effected by flooding, the radar classification map image from SIR-B was geometrically registered and added to the classified Landsat MSS map image. Prior to their addition, the two binary classification maps were renumbered so that the new combined map product would show changes in land cover over time as a result of flood boundary movement (Plate 4c, Table 4). The main objective of the merger of the radar data with the Landsat MSS data was to take advantage of the temporal difference between the two data sets. The primary strength of the MSS data in this case was that it was acquired during a time of flooding and showed inundation areas. The digital merger of the two image classifications allowed for the separation of the Village/Agriculture class on the MSS data by comparison to the radar, and provided a basis for making areal estimates as to which land-cover categories were inundated at the time of the September MSS overpass. Calculation of inundation subsidence was determined for the 16-day period between the time of the MSS acquisition and the SIR-B overflight. The calculation was made by assigning a reference value to the land-cover classes on both the MSS and SAR classification images, geometrically registering the map images to one another, and then adding them together to form a new combined map image. Because the land-cover classes on the radar map image were more accurate and most of the flooding was prevalent at the time of the MSSacquisition, the new class assignments for the merged data set were made using the radar as a land-cover reference and the MSS as a flood boundary delimiter. From this merged data product, measurements were made defining the total areal extent of the flooding present at the time of the MSS acquisition and the area contributions made by each land-cover class. This allowed for damage assessment to proceed by making estimates of how much infrastructural damage (number of hectares of village flooded) and agricultural damage (number of hectares of agricultural land affected by floods) may have occurred as a result of the flood levels experienced at the time of the MSS overpass. A simple linear model associating areal inundation measurements with river level was made by taking the difference between measurements from a river level guage positioned at Chandpur on the Ganges near the center of the study area at the time of the MSS and the SIR-B data acquisitions. Total flood area and flood areas associated with each land-cover class could be plotted as a function of river guage level. According to the measurements made by the merged SIR/BLandsat data, approximately 63,000 hectares were flooded by river overflow on 27 September 1984. By 12 October 1984, river induced flooding dropped to virtual zero, which translates to a rate of 4200 hectares of land emerging each day. River guage measurements made for these two dates in the Ganges River at Chandpur indicated river levels of 4.46 and 3.88 metres, respectively. This constitutes a drop rate of 3.86 centimetres per day. A simple linear plot comparing the land emergence and river level drop rates between these two dates indicates that approximately 1088 hectares of

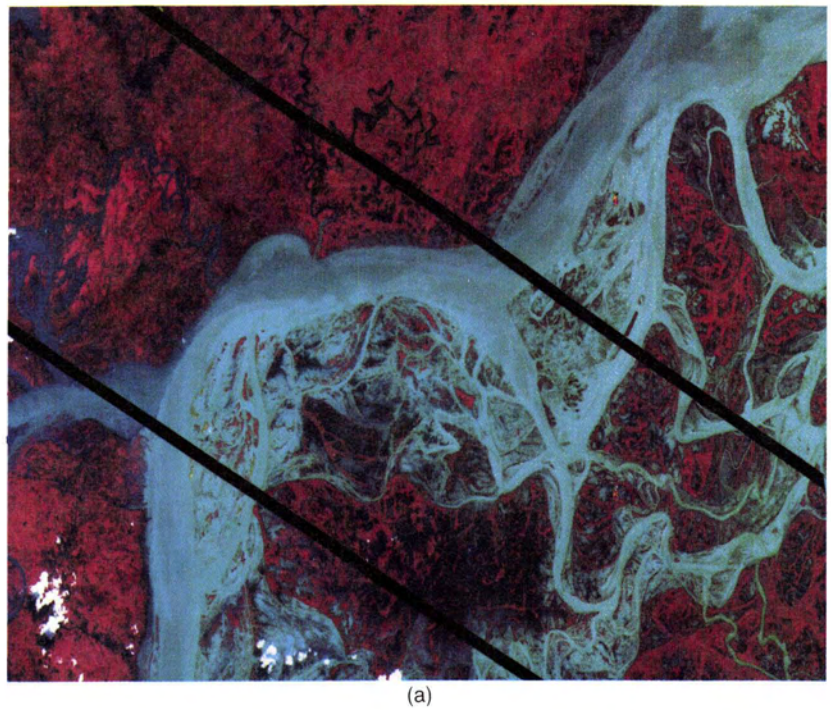

(a)

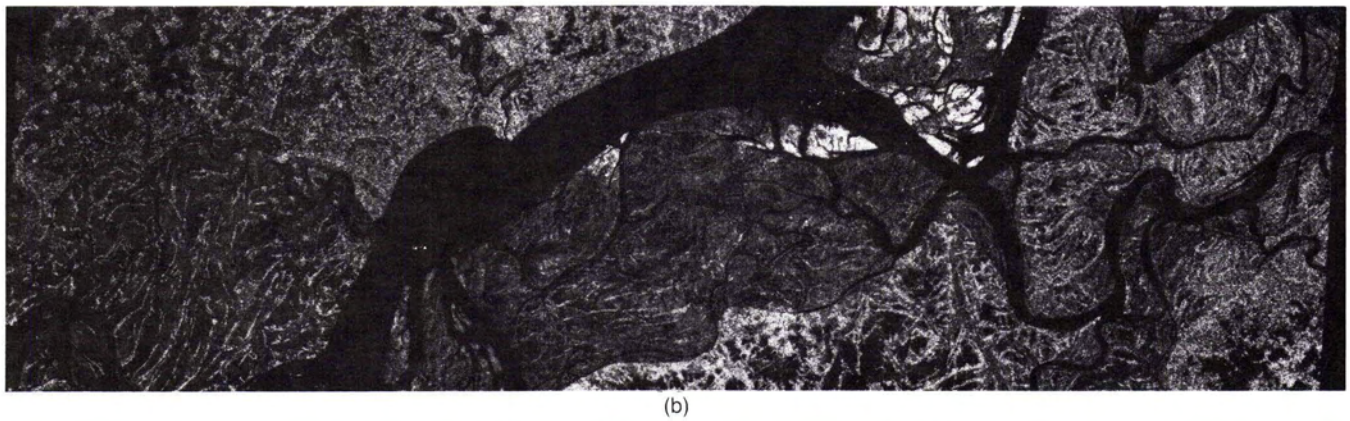

(b)

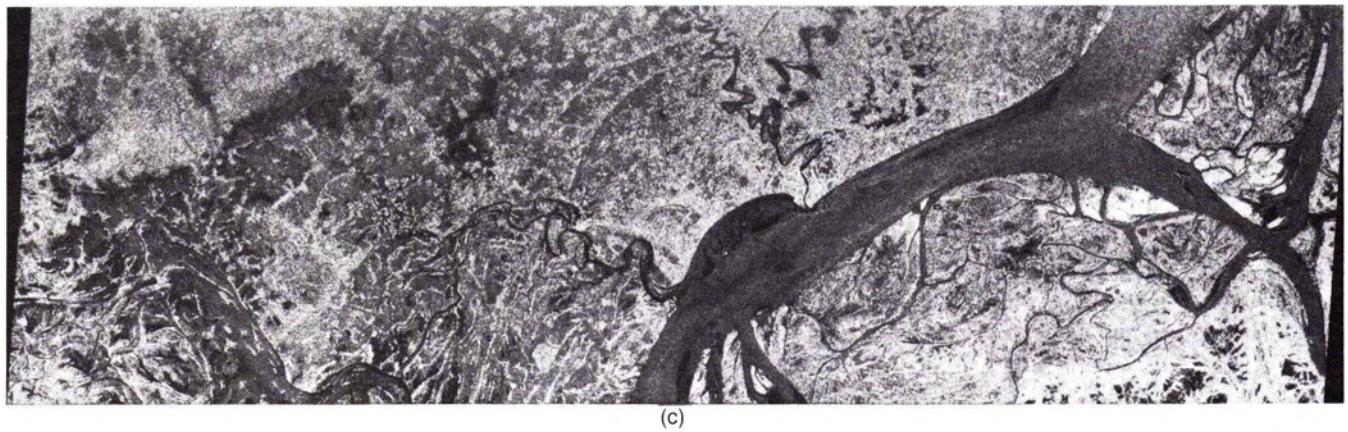

(c)

PLATE 2. (a) Landsat MSS false color infrared composite and (b) SIR-B radar image of the Chandpur survey area. The Landsat scene was acquired 27 Sept. 1984 with rice crops still present and monsoon and storm induced flooding still in effect. The radar image was acquired 15 days later after the flood waters had receeded. (c) SIR-B image of Chandpur area taken during storm activity. Turbulent water causes higher radar backscatter making automated land and water separation difficult.

land may be expected to emerge (given similar rainfall conditions, etc.) for every centimeter drop in river level between 4.46 and 3.88 meters.

Albeit, this is a simple example; however, it is still important in its implications for future modeling because additional data can further quantify the relationship between river level and land inundation/emergence over a broader range of conditions. The incorporation of weather data into the model would further

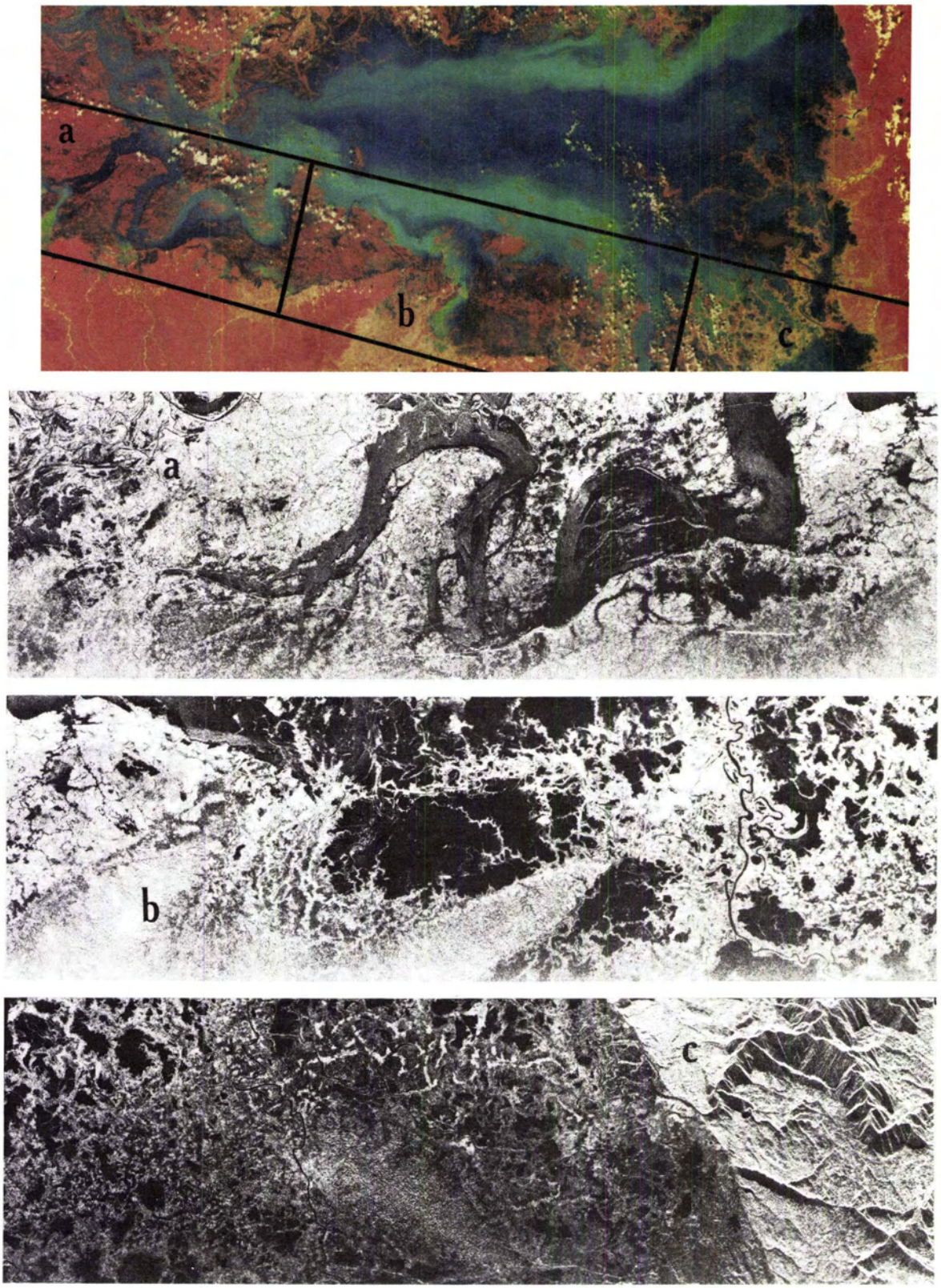

PLATE 3. (top image) Landsat MSS false color composite, acquired 27 Sept. 1984, of Mymensingh Depression area showing extensive flooding. Corresponding SIR-B images taken 15 days later are shown for comparison (bottom three images). Black areas on radar images denote relatively non-turbulent standing water. Dark gray areas represent surface water undergoing wind induced turbulence from a storm front that moved in during SIR-B overflight. The river shown in the first SIR-B image is typically dry during the winter months.

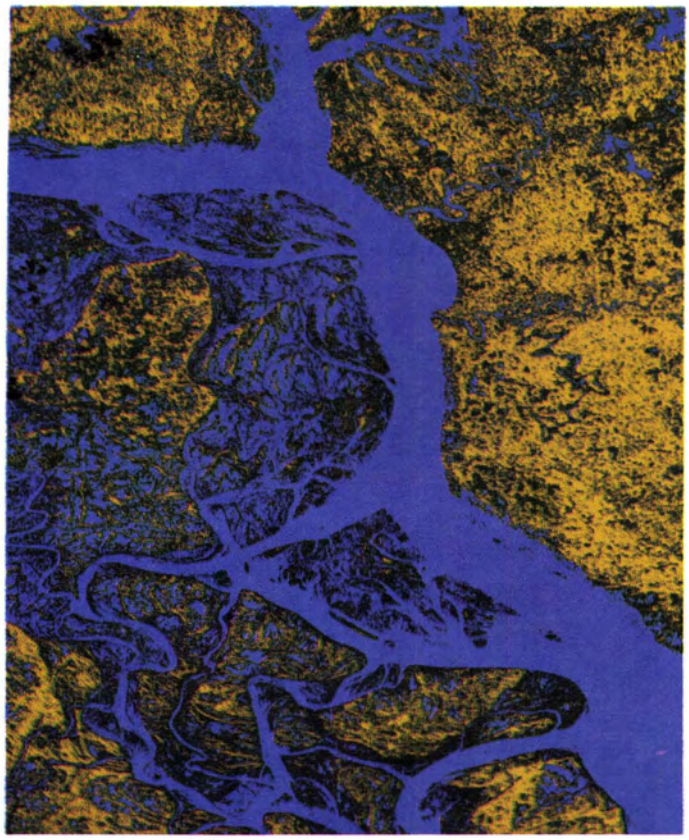

(a)

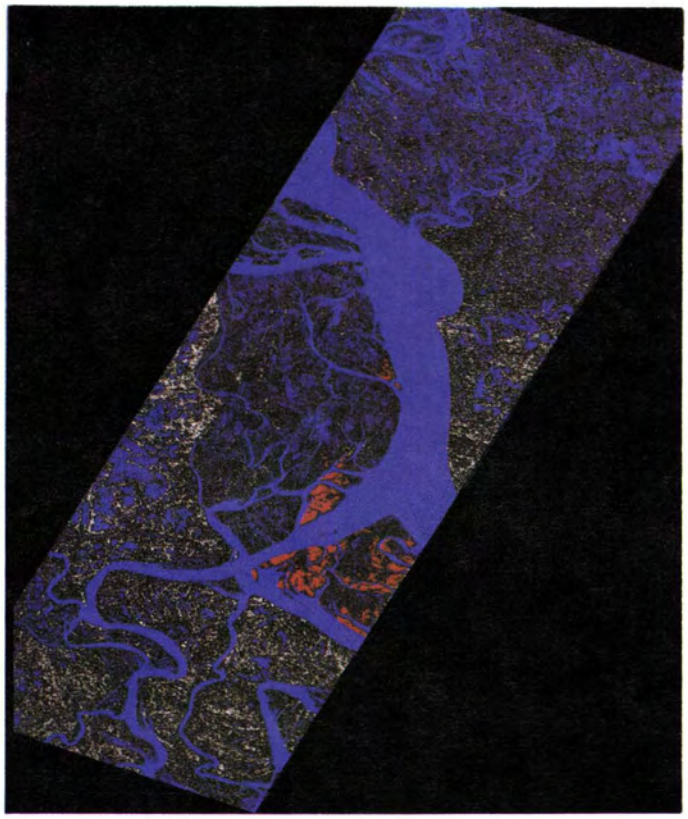

(b)

(c)

PLATE 4. (a) Landsat MSS land-cover classification of Chandpur survey area showing Agriculture and Village areas (yellow and green), Flooded Land (dark gray), and Surface Water (blue). (b) Spatially filtered and density sliced L-band radar image of Chandpur site showing Village/Infrastructure (white), Agricultural Land (Gray), Surface Water (blue), and Scrub Vegetation (orange). (c) This image represents the combined Landsat MSS and SIR-B radar image classification product of Chandpur area. In the center strip, radar data overlain on the Landsat scene aided in the separation of land-cover categories and provided a means of classifying flood damage. Non-flooded Agricultural Land (yellow and green), Non-flooded Village and Infrastructure (red), Village/Infrastructure (white) and Agricultural Land flooded 27 Sept. 1984, (purple and light blue). Light blue areas only recently emerged whereas the purple areas have new crop growth started. Non-turbid non-flood stage water shows as black.

refine its accuracy and provide for a very powerful tool for flood prediction, monitoring, and damage assessment.

CONCLUSIONS AND REMARKS

L-band radar imagery can be a very useful tool for monitoring flood boundaries and other surface features during the monsoon. Radar's ability to penetrate cloud cover and rain permit the acquisition of image data actually during the monsoon period and/or during storm precipitation. The physical nature of radar imaging also permits and clear definition of nonturbulent

flood and irrigation waters, and good separation from the surrounding landscape. This latter characteristic proved especially useful for clearly identifying raised dike works and housing units and separating them from the agricultural fields. This ability is of particular significance to countries that rely to a large extent on flood irrigation agricultural practices.

The L-band radar and the techniques used here to analyze it did suffer from limitations concerning land-use/land-cover mapping. Turbulent water, mature agricultural crops, and urban land covers still cannot be separated or discriminated to a high degree of accuracy. Future use of radar systems, however, may overcome many of these problems. By 1990 the availability of radar data from European, Canadian-American, and Japanese SAR satellites will permit more accurate classification through the use of multiple frequency, multiple aspect, and multiple polarization radar data sets.

As satellite-acquired SAR data becomes available worldwide in the 1990's, the use of SAR and multispectral imagery, multiple data merging techniques, and the incorporation of ground acquired point data can be used as a powerful tool for measuring and monitoring flood progression and damage by identifying and quantifying the land areas experiencing stress and determining the potential impact based on land-use/land-cover identification. The example shown here was a simple one performed to a great extent "offsite." An "in country" analysis would benefit from better and more plentiful ground information, and, with the availability of higher resolution multispectral data (i.e., Landsat TM and SPOT), more detailed and accurate land-cover classifications could be generated.

REFERENCES

Berg, A., and J. M. Gregiore, 1983. Use of Remote Sensing Techniques for Rice Production Forecasting in West Africa, (Mali and Guinea: Niger-Bani Project). *ESA Satellite Remote Sensing for Developing Countries,* Ispra, Italy, pp. 161–168.

Bhavsar, P. D., 1984. Review of Remote Sensing Applications in Hydrology and Water Resources Management in India. *(COSPAR, IUGS, COSTED, and United Nations, Workshops on Remote Sensing from Satellites, 1st and 9th, and Topical Meeting, Graz, Austria, June 25 - July 7, 1984) Advances in Space Research,* Vol. 4, No. 11, pp. 193–200.

Congalton, R. G., R. G. Oderwald, and R. A. Mead, 1983. Assessing Landsat Classification Accuracy Using Discreet Multivariate Analysis Statistical Techniques. *Photogrammatric Engineering and Remote Sensing,* Vol. 49, No. 12, pp. 1671–1678.

Imhoff, M. L., and M. H. Story, 1986. Forest Canopy Characterization and Vegetation Penetration Assessment with Space-Borne Radar. *IEEE Trans. on Geoscience and Remote Sensing,* GE-24, No. 4.

Lowry, R. T., N. Mudry, and E. J. Langham, 1979. A Preliminary Analysis of SAR Mapping of the Manitoba Flood, May 1979, Satellite Hydrology; *Proceedings of the Fifth Annual William T. Pecora Memorial Symposium on Remote Sensing,* Sioux Falls, South Dakota.

Krohn, M. D., N. M. Milton, and D. B. Segal, 1983. SEASAT Synthetic Aperture Radar (SAR) Response to Lowland Vegetation Types in Eastern Maryland and Virginia. *Journal of Geophysical Research,* Vol. 88, No. C3, pp. 1937–1952.

MacDonald, H. C., W. P. Waite, and J. S. Demarcke, 1980. Use of Seasat Satellite Radar Imagery for the Detection of Standing Water Beneath Forest Vegetation, *Proceedings of Amer. Soc. of Photogrammetry Ann. Tech. Meeting,* Niagara Falls, New York, pp. RS-3-B-1 to RS-3-B-13.

Ormbsy, J. P., J. P. Blanchard, and A. J. Blanchard, 1985. Detection of Lowland Flooding Using Active Microwave Systems, *Photogrammetric Engineering and Remote Sensing,* Vol. 51, No. 3., pp. 317–328.

Ruangsiri, P., R. Sripumin, S. Polngam, P. Kanjanasuntorn, and S. Wongparn, 1984. State of Flooding in the Mun-Chi River Basin Area, N. E. Thailand by Digital Landsat Data Analysis. *Report: Remote Sensing Division, National Resource Council of Thailand.* Bangkok, Thailand.

Rashid, H. E., 1981. *An Economic Geography of Bangladesh.* University Press Limited Dhaka, Bangladesh.

Thomson, K. P. B., and C. Prevost, 1983. Tracking of Water Levels and Mapping of Flood Plains by Satellite. *First International Training Seminar on Remote Sensing Applications to Operational Agrometeorology in Semi-Arid Countries, ESA,* Paris, pp. 31–35.

Waite, W. P., and H. C. MacDonald, 1971. Vegetation Penetration with K-Band Imaging Radars, *IEEE Trans. on Geosci. Electron.,* Vol. GE-9, No. 3., pp. 147–155.

Waite, W. P., H. C. MacDonald, V. H. Kaupp, and J. S. Demarche, 1981. Wetland Mapping With Imaging Radar, *Proceedings of 1981 International Geoscience and Remote Sensing Symposium* 8–10 June, Washington, D.C., IEEE Geoscience and Remote Sensing Society.

(Received 11 July 1986; revised and accepted 21 November 1986)

The Second Industrial and Engineering Survey Conference

University College London
2–4 September 1987

The 2nd Industrial and Engineering Survey Conference has been arranged under the joint auspices of the International Society for Photogrammetry and Remote Sensing (ISPRS) Commission V and the International Federation of Surveyors (FIG) Commission 6. The time is now appropriate to bring together interests in large-scale metrology, industrial and engineering surveying, and close-range photogrammetry in order to assess recent advances in this area. All authors of papers at the Conference have been specially invited. A wide range of industrial, commercial, and academic backgrounds will be represented.

Organization of many aspects of the conference has been shared with colleagues at The City University, University of Surrey, Imperial College of Science and Technology, and South Bank, North East London, and Portsmouth Polytechnics.

For further information please contact

Dr. J. C. Iliffe
University College London
Gower Street
London WC1E 6BT
United Kingdom
Tele. 01-387 7050, ext. 2733